



Trade Science Inc.

ISSN : 0974 - 7486

Volume 9 Issue 6

Materials Science

An Indian Journal

Full Paper

MSAIJ, 9(6), 2013 [227-233]

Responses to indentation and to impedance spectroscopy of plastically compressed steels. Part 2: Case of a Fe-Ni-Cr steel

Pierre-Yves Girardin¹, Adrien Frigerio¹, Patrice Berthod^{2*}

¹Lycée Henri Loritz, 29 Rue des Jardiniers 54000 Nancy, (FRANCE)

²Institut Jean Lamour (UMR CNRS 7198), department CP2S, team “Surface and Interface, Chemical Reactivity of Materials”, University of Lorraine, B.P. 70239, 54506 Vandoeuvre-lès-Nancy, (FRANCE)

E-mail: patrice.berthod@univ-lorraine.fr

ABSTRACT

As in the first part of this study impedance spectroscopy was used in this second part to characterize the influence of permanent deformation in compression on the corrosion behaviour, in the same sulphuric acid solution, of a second model iron-based alloy – a ternary Fe-Ni-Cr alloy, base of many stainless austenitic steels – always for the two main orientations of surface with respect to the deformation axis. Preliminary to the EIS experiments, XRD runs and Vickers indentations showed the same effects of the plastic deformation in compression on diffraction patterns and on hardness. The Nyquist plots obtained were also similar to semi-circles and the corresponding charge transfer resistances and double layer capacitance were determined. In contrast with what was observed for pure iron in the same conditions (except the deformation rates really achieved because of the much higher strength of the simplified austenitic stainless steel studied here by comparison to pure iron) the transfer resistance rather tended here to decrease when the permanent compression deformation increased, and to be higher for the perpendicular orientation than for the parallel orientation.

© 2012 Trade Science Inc. - INDIA

KEYWORDS

Stainless austenitic steel;
Compression;
Plastic deformation;
Hardness;
Corrosion;
Impedance spectroscopy.

INTRODUCTION

As already explained in the first part of this work^[1], many metallic pieces are plastically deformed when they are shaped during their fabrication or when they have been subjected to intense mechanical stresses during their use, and therefore they may present general or local modifications of their surface reactivity, notably when immersed in aqueous solutions with in this case the possibility of galvanic coupling in addition. These

are the reasons of numerous studies about the effect of a plastic deformation on the corrosion behaviour of various metals and alloys, and notably ferrous alloys^[2-5], in some cases specified by using impedance spectroscopy^[6-10].

The purpose of this second part^[1] of this study, which began with the case of pure iron, is to use the same methodology for studying the effect of different rates of plastic deformation of a Fe-Ni-Cr ternary alloy, base model of many austenitic stainless steels, on its corro-

Full Paper

sion behaviour characterized by EIS measurements.

EXPERIMENTAL

Elaboration of the as-cast steel cylinder and compression runs

As earlier done for iron in the first part of this study, foundry was used to elaborate ingots of about 40g of the considered alloy before confectioning the electrodes. Parts of pure iron, pure nickel and pure chromium (> 99.9 wt.%) were melted together by High Frequency induction melting (CELES) in an inert atmosphere of pure Argon (300mbars). To obtain samples with a shape easy to perform compression and to prepare electrodes with either a surface parallel to the deformation direction or a surface perpendicular to this direction, it was here too preferred to aspire the alloy from the levitating ball of molten alloy, in a silica tube in which the alloy can solidify as a full cylinder with a diameter of near 10 millimetres. For 40g of alloy the length obtained was of about four centimetres long since a part of the alloy remained outside the tube. Here too the solidified cylinder was cut in several parts to perform the compressions (here too using the MTS-RF/150 testing machine). As for the iron samples in the first part of the study^[1], the targeted deformation rates were -12.5%, -25% and -40%. Because of the higher strength of the Fe-Ni-Cr steel (by comparison to pure iron) the obtained permanent deformation obtained here were lower: -3.08%, -10.7% and -17.6% only. The initial dimensions and the deformations achieved with the compression runs are given in TABLE 1, while the yield strengths noted on the compression curves are displayed in TABLE 2. These last values, significantly higher than the ones previously obtained for similar samples of pure iron^[1], mean that the austenitic steel considered in this second part of this study is –logically much more mechanically resistant than the ferritic iron samples.

TABLE 1 : Values of the diameters and heights of the sample before and after compression test (without stress applied, measured using a numeric caliper).

FeNiCr alloy	Low compression	Medium compression	High compression
Initial diameter (mm)	10.74	10.76	10.72
Initial height (mm)	9.80	12.34	14.03
Deformation (%)	-3.08	-10.7	-17.6

TABLE 2 : Values of the yield strength in compression.

FeNiCr alloy	Low compression	Medium compression	High compression
Yield strength (MPa)	173	218	179

Preparation of the specific samples for metallographic characterization and for the electrodes

The as-cast sample and the three deformed samples were here too cut using a Buelher Isomet 5000 precision saw, following a method which allows obtaining metallographic samples and electrodes exposing a surface being either parallel or perpendicular to the deformation axis (e.i. the cylinder axis). The obtained parts of the two types were embedded in a cold resin (ESCIL: CY230 and HY 956 products), after having been connected to a plastic-covered copper electrical wire in the case of the electrode. The surfaces of all the samples, metallographic and electrode, were thereafter polished with SiC papers up to 1200-grit, then to mirror-state with 1 µm-particles pastes for the metallographic sample.

Microstructure characterization and Vickers indentations

The metallographic samples were first subjected to X-Ray Diffraction using a Philips X'Pert Pro diffractometer (wavelength Cu K α) for specifying the crystalline network of the as-cast and the deformed samples. Second, they were subjected to Vickers indentations using a Testwell Wolpert machine (load: 10kg). Three indentations were realized for each of the eight metallographic samples (4 deformation levels including the not deformed state \times 2 orientations), for calculating the average value and the standard deviation one.

Impedance spectroscopy runs

The EIS runs were performed in the same electrolyte as for the iron samples^[1] (sulphuric acid aqueous solution: H₂SO₄ 2N), using a {three electrodes}-cell with the studied sample as working electrode, a Saturated Calomel Electrode (SCE) as reference for potentials, and a graphite rod as counter electrode. The potentiostat was an Ametek one, driven by the Versastudio software. In each case the Open Circuit Potential was measured first, and thereafter the applied E varied alternatively between E_{ocp} -10mV to E_{ocp} +10mV with a decreasing frequency (100,000Hz

down to 1Hz). This was repeated five times: at $t=1$ minute after immersion, $t=6$ min, $t=11$ min, $t=16$ min and $t=21$ min.

RESULTS AND DISCUSSION

Microstructure characterization

The X-ray diffraction patterns presented in Figure 1 (parallel orientation, all deformation states) and in Figure 2 (perpendicular orientation, all deformation states) show that the steel samples are not wholly austenitic but are composed of both austenitic and ferritic phases, for the three compressed states as well as for the not-compressed one. In addition it appears that the higher the deformation rate the more numerous the diffraction peaks really visible for the parallel orientation, while it is the contrary for the perpendicular orientation. These are the same observations as previously done for the iron samples^[1].

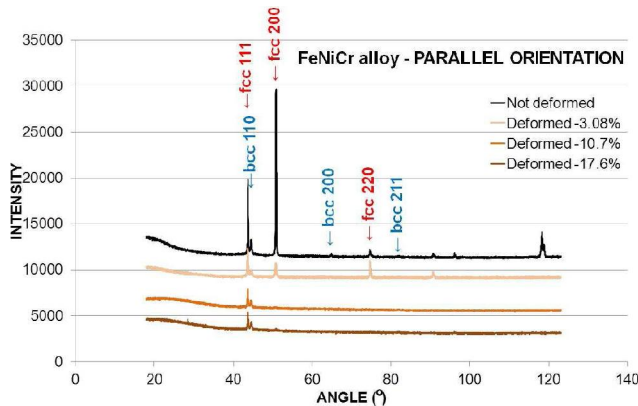


Figure 1 : XRD patterns obtained for the not-deformed state and for the three deformed states (parallel orientation).

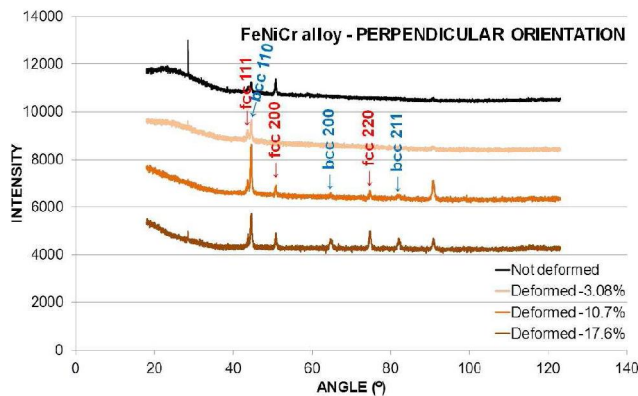


Figure 2 : XRD patterns obtained for the not-deformed state and for the three deformed states (perpendicular orientation).

Vickers indentations

Concerning the evolution of the hardness with the deformation rate (illustrated by the two curves superposed in Figure 3), one finds again (i.e. as for the iron samples^[1]) the same well-known increase in hardness with the deformation rate (here about +150Hv points for 17.6% of deformation in compression) with again a tendency to slightly higher values for the perpendicular orientation by comparison with the parallel orientation.

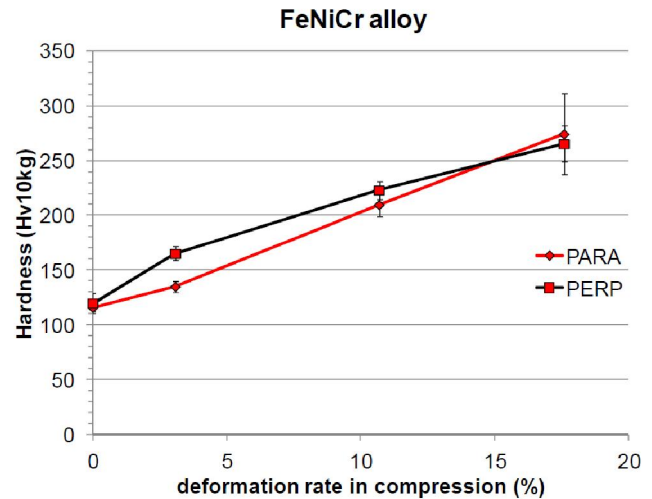


Figure 3 : Evolution of the Vickers hardness versus the deformation rate and for the two orientations.

Impedance spectroscopy

The EIS results are displayed as Nyquist diagrams $\{Z_{\text{imag}} = f(Z_{\text{real}})\}$ superposed for the two orientations in the same graph for the same compressed state, in Figure 4 for the not-compressed sample, in Figure 5 for the sample compressed at -3.08%, in Figure 6 for the sample compressed at -10.7% and in Figure 7 for the sample compressed at -17.6%. The Nyquist semi-circles obtained for all samples and for all times are all semi-circles more or less flattened (i.e. semi-ellipsoids). The radii of these semi-circles generally increase with time, with an exception: the first semi-circle ($t=1$ min) for the perpendicular orientation of the {-10.7%}-deformed sample was found as curiously great. This deformation rate leads to other curious behaviours as especially small radii at all times for the parallel orientation, by comparison to the other deformed states for the same orientation, while the semi-circles obtained for the {-10.7%}-deformed sample for the perpendicular orientation are more conform to the ones obtained

Full Paper

for the other deformation states for the same orientation. Thus, if the parallel orientation for the $\{-10.7\}$ -deformed sample is taken out the Nyquist curves under consideration it appears that, for all the other cases, the semi-circles become greater with time, with a radius for the parallel orientation higher than for the perpendicular orientation for the two lowest deformation rates (0% and -3.08%) and for the parallel orientation much lower than for the perpendicular orientation for the highest deformation rate (-17.6%). It is true that this should be also verified for the $\{-10.7\}$ -deformed state.

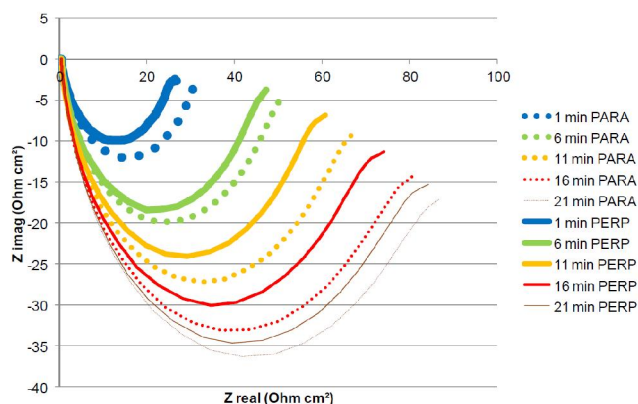


Figure 4 : Nyquist plot of the EIS results for the not-deformed sample for the two orientations.

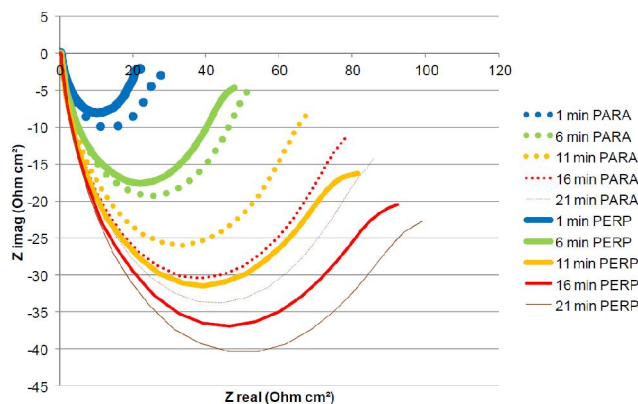


Figure 5 : Nyquist plot of the EIS results for the sample deformed at -3.08% for the two orientations.

The semi-circular shape (with, it is true, maybe a tendency to evaluate to a Warburg straight line on the low frequencies side, except for the -17.6% deformation) let think that the classical electrokinetic scheme already reminded in the first part of this study^[1] is valid here too. As previously done in the first part of this work, it was tried to assess the values of the electrolyte resistance, of the transfer resistance and of the double layer capacitance. Concerning the resistance of the electro-

lyte (R_{el} , TABLE 3), it is rather constant and logically does not depend on the orientation and on the deformation rate, even if it seems that it remains for the perpendicular orientation slightly lower than for the parallel orientation for the not-deformed state and, in contrast, slightly lower in the perpendicular case than in the parallel case for the two highest deformation rates. Concerning the transfer resistance it is obvious that R_t increases with time for all deformed states and for the two orientations, which let think to the progress of a passivation phenomenon. It appears too, for the not-deformed state and also for the $\{-3.08\}$ -deformed state for the first minutes, that R_t is slightly higher for the parallel orientation than for the other one, while there is the opposite for the $\{-3.08\}$ -deformed state for the last minutes as well as for the two highest deformations. In addition, except the particular behaviour of the $\{-10.7\}$ -deformed samples, the R_t values for a given time and a given orientation, decreases when the deformation increases; this is particularly obvious by comparing the $\{0\}$ - and $\{-3.08\}$ -deformed states on the one hand and the $\{-17.6\}$ -deformed state on the other hand.

TABLE 3 : Value of the electrolyte resistance versus the deformation rate and the orientation.

R_{el} (Ohm cm ²)	Orientation	t=1 min	t=6 min	t=11 min	t=16 min	t=21 min
Not deformed	PARA	0.372	0.401	0.411	0.414	0.422
	PERP	0.419	0.449	0.446	0.450	0.457
-3.08%	PARA	0.452	0.481	0.496	0.484	0.490
	PERP	0.406	0.427	0.439	0.444	0.451
-10.7%	PARA	0.431	0.458	0.472	0.481	0.485
	PERP	0.461	0.469	0.493	0.498	0.494
-17.6%	PARA	0.342	0.366	0.380	0.370	0.385
	PERP	0.456	0.488	0.507	0.494	0.513

TABLE 4 : Value of the transfer resistance versus the deformation rate and the orientation.

R_t (Ohm cm ²)	orientation	t=1 min	t=6 min	t=11 min	t=16 min	t=21 min
Not deformed	PARA	29.3	46.1	61.3	75.6	77.9
	PERP	23.6	42.8	55.2	66.4	76.6
-3.08%	PARA	23.9	45.3	62.4	72.9	79.3
	PERP	19.3	40.9	70.3	82.0	87.7
-10.7%	PARA	19.9	27.9	34.4	37.6	41.0
	PERP	143.7	57.4	74.2	91.3	104.0
-17.6%	PARA	14.8	23.3	27.4	27.6	28.5
	PERP	20.0	32.1	36.0	36.1	35.4

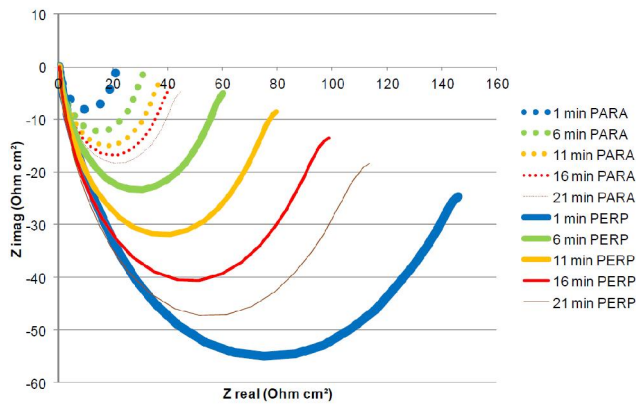


Figure 6 : Nyquist plot of the EIS results for the sample deformed at -10.7% for the two orientations.

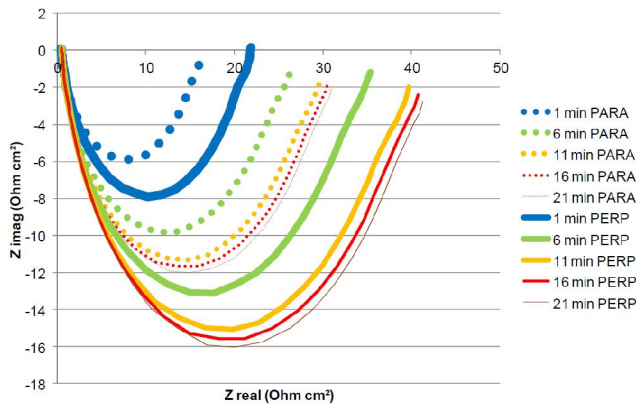


Figure 7 : Nyquist plot of the EIS results for the sample deformed at -17.6% for the two orientations.

TABLE 5 : Value of the frequency corresponding to the nyquist circle summit versus the deformation rate and the orientation.

f circle summit (Hz)	orientation	t=1 min	t=6 min	t=11 min	t=16 min	t=21 min
Not deformed	PARA	50.1	31.6	20.0	15.8	12.6
	PERP	63.1	31.6	25.1	20.0	15.8
-3.08%	PARA	79.4	25.1	20.0	15.8	12.6
	PERP	79.4	31.6	15.8	12.6	10
-10.7%	PARA	63.1	39.8	39.8	31.6	25.1
	PERP	12.6	25.1	20.0	15.8	15.8
-17.6%	PARA	100	50.1	39.8	39.8	31.6
	PERP	100	50.1	39.8	31.6	31.6

By noting the values of the frequency corresponding to each semi-circle summit (TABLE 5) it is possible to determine the values of the capacitance of the double layer (as earlier done for pure iron in the first part of this work^[1]). The values obtained for C_{dl} , displayed in TABLE 6, tends to slightly increase with time and to be higher for the parallel orientation than for the perpendicular one, for the two highest deformation states. This

is in contrast not so clear for the two lowest deformation rates, for which the values are rather close to one another for the two orientations. To finish, concerning the Open Circuit Potential recorded preliminary to each EIS experiment (TABLE 7), there is seemingly no real dependence, neither on the deformation rate, nor on the orientation.

TABLE 6 : Value of the double layer capacitance versus the deformation rate and the orientation.

C_{dl} (10^{-3} F)	orientation	t=1 min	t=6 min	t=11 min	t=16 min	t=21 min
Not deformed	PARA	0.680	0.686	0.818	0.835	1.020
	PERP	0.672	0.738	0.721	0.755	0.824
-3.08%	PARA	0.528	0.879	0.803	0.865	1.002
	PERP	0.652	0.774	0.898	0.969	1.141
-10.7%	PARA	0.797	0.901	0.731	0.842	0.972
	PERP	0.553	0.693	0.675	0.691	0.607
-17.6%	PARA	0.675	0.857	0.915	0.910	1.110
	PERP	0.501	0.622	0.699	0.876	0.892

TABLE 7 : Evolution of the open circuit potential versus time for the different deformation rates and for the two orientations.

E_{ocp} (/HNE, mV)	orientation	t=1 min	t=6 min	t=11 min	t=16 min	t=21 min
Not deformed	PARA	-220	-231	-225	-215	-209
	PERP	-218	-231	-226	-220	-231
-3.08%	PARA	-198	-215	-213	-211	-209
	PERP	-202	-212	-197	-194	-193
-10.7%	PARA	-225	-236	-235	-232	-229
	PERP	-104	238	-227	-222	-218
-17.6%	PARA	-225	-228	-226	-224	-222
	PERP	-225	-228	-226	-224	-222

General commentaries

First the compression tests performed on this Fe-Ni-Cr alloy showed that this one was significantly more mechanically resistant than pure iron elaborated in exactly the same conditions, despite that it is only a simple ternary alloy and then not so sophisticated as a commercial austenitic stainless steel. This did not permit obtaining permanent deformation states as for pure iron for the performances of the testing machine (tests were interrupted when the applied force reached about 70kN, as for the pure iron samples of the first part of this work^[1]). This can be illustrated by the values of yield strength obtained which are here twice or more the ones

Full Paper

obtained for pure iron. The better mechanical behaviour of this ternary alloy also concerns hardness the values of which are twice the ones obtained for pure iron. However the matrix of the present ternary alloy was not totally austenitic since the XRD spectra clearly showed the co-existence of ferrite and austenite. Concerning these results, the same phenomenon as met for pure iron concerning the dependence of the spectra on both the orientation and the deformation rate, was also encountered for the Fe-Ni-Cr alloy: the disappearance of some of the diffraction peaks with the compression rate for the parallel orientation and the inverse evolution with the deformation rate too for the perpendicular orientation. This double evolution, which remains to be confirmed with additional results, remains to be understood, as well as the dependence of the same XRD spectra on the orientation for the not-deformed samples for which an uniaxial deformation by compression cannot be responsible of such difference for the two orientation. In this latter case the radial growth during solidification may be a possible explication.

Concerning now the results of impedance spectroscopy it appeared that all the Nyquist plots are similar to the semi-circles which are obtained when the electrokinetic model composed of a resistor (electrolyte resistance) is mounted in series with another resistor (transfer resistance) mounted in parallel with a capacitor (double layer capacitance), although the semi-circles obtained here must be rather qualified as semi-ellipsoids and the low frequency parts seem to present a beginning of Warburg straight line. An interesting observation concerning this latter point is that this beginning of Warburg-type straight line, which existed for the not-deformed samples and for the low-deformed ones, did not exist anymore for the highest deformation rate. If no real difference was observed neither for the electrolyte resistance (the distance between the working electrode and the auxiliary one was sensibly the same and then no different values for R_{el} was expected) nor for the Open Circuit Potential, it appeared that the charge-transfer resistance was more interesting to follow. Its increase with time seemed showing that this alloy highly alloyed with chromium was passivating, may be more or less quickly depending on the deformation rate (at each time lower R_t values for the highly compressed samples by comparison to the not- or few-

deformed states) and on the orientation especially for the highest deformation rate (R_t higher for the perpendicular orientation by comparison with the parallel one). The corrosion resistance is then, after a same immersion duration, lowered by a plastic deformation in compression and this more for the parallel orientation than for the perpendicular one. A dependence on both the deformation rate and the orientation seems existing concerning the double layer capacitance but maybe less evident than for the transfer resistance.

CONCLUSIONS

If the effects of the mechanical deformation in compression on the XRD patterns and on the hardness were the same for this ternary Fe-Ni-Cr alloy as for the pure iron studied in the first part of this work, the dependence of the transfer resistance is here inverse by comparison with pure iron (in the same electrolyte H_2SO_4 2N). However, the deformation rates achieved for the two types of metallic sample were not the same and such comparison needs to be verified with additional EIS experiments performed on iron samples less deformed in compression and on Fe-Ni-Cr alloy more deformed (using samples with the same size but a strongest testing machine). It may be also interesting to deeper investigate the behaviours of these compressed samples for lower frequencies (down to 0.01 Hz for example) to further study the effect of compression on the Warburg part possibly existing in the electrokinetic model, and also to extend the study to other electrolytes.

REFERENCES

- [1] A.Frigerio, P.Y.Girardin, P.Berthod; Materials science, An Indian Journal, Submitted.
- [2] E.Conrath, P.Berthod; Materials science, An Indian Journal, **9(3)**, 107 (2013).
- [3] B.Mazza, P.Pedefferri, D.Sinigaglia, U.Della Sala, L.Lazzari; *Werstoffe und Korrosion*, **25**, 239 (1974).
- [4] B.Mazza, P.Pedefferri, D.Sinigaglia, A.Cigada, L.Lazzari, G.Re, D.Wenger; *Journal of the Electrochemical Society*, **123**, 1157 (1976).
- [5] V.I.Storonskii; *Teploenergetika*, **33**, 615 (1986).
- [6] M.Sanchez, H.Mahmoud, M.C.Alonso; *Journal of*

- Solid State Electrochemistry, **16(3)**, 1193 (**2012**).
- [7] J.J.Shi, W.Sun; Fushi Kexue Yu Fanghu Jishu, **23(5)**, 387 (**2011**).
- [8] X.Li, Y.Wang, C.Du, B.Yan; Journal of Nanoscience and Nanotechnology, **10(11)**, 7226 (**2010**).
- [9] A.Hemmasian-Ettefagh, M.Amiri, C.Deaghanian; Materials Performance, **49(3)**, 60 (**2010**).
- [10] Y.Ma, Y.Li, F.Wang; Corrosion Science, **51**, 997 (**2009**).